

MAST 602

Lecture 9 Tides and long-period waves

Introduction

In this lecture we consider waves that are:

- Shallow-water, long waves
- Non-dispersive
(i.e., phase velocity = group velocity)
- Long period, long wavelength

$$c = \sqrt{gh}$$

Examples of such waves are

- tsunami
- seiches
- internal waves
- tides

Tsunami

Tsunami are generated by earthquakes
(they're sometimes called
"seismic sea waves")

They are shallow-water waves;

Knowing the depth of the ocean,
their time of arrival can be predicted

Tsunami sometimes produce
devastating effects on coastlines

With no friction,
the energy flux, vE , = constant

Recall that $E = \frac{1}{2} \rho g A^2$

and that $v = \sqrt{gh}$

$$\text{so that } h \propto \frac{1}{A^4}$$

Thus, as the water depth shoals
coming onshore, the height of
the tsunami wave increases:

h water depth	A wave amplitude	L wavelength	T period
20 m	15 m		
4000 m	4 m	120 km	10 min

On the other hand, tsunami are generally undetected at sea

The sea-surface slope associated with a tsunami $\sim 1/12,000$

Such a slope is undetectable, so although tsunami can create great damage when they come on shore, they aren't noticed by ships at sea

The most effective way to track tsunami and warn of their arrival is to watch for earthquakes and calculate the time of arrival of a possible tsunami on distant shores

The Pacific Ocean is a region particularly susceptible to earthquakes and thus to tsunami

The Pacific Tsunami Warning System, (Honolulu) is operated by Pacific-rim countries to give warning of arriving tsunami.

Seiches

A seiche is a resonant oscillation of a lake or harbor (or a bathtub), much like vibration in an organ pipe

Fig 10- 1 Domestic seiche

Calvin & Hobbes

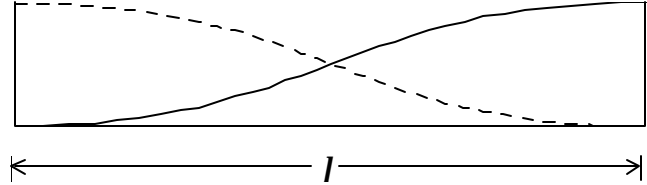
Warning! Do not attempt this experiment at home. It should only be done by professionals under controlled conditions.

For a standing wave in a closed channel,
 the channel length, l ,
 equals a half wavelength, $\Lambda/2$.

Then,

$$c = \frac{\Lambda}{T} = \frac{2l}{T} = \sqrt{gh}$$

$$T = \frac{2l}{\sqrt{gh}}$$



The period of oscillation depends
 on the depth of water and
 on the length of the channel

In general,

$$T = \frac{2l}{n\sqrt{gh}}, \quad \text{for } n = 1, 2, 3, \dots$$

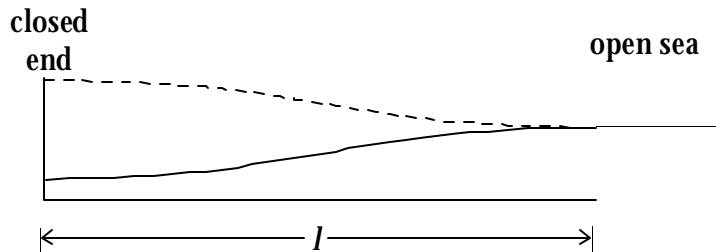
Suppose the channel is open at one end
 Then a node occurs at the channel opening
 and an antinode occurs at the channel end.

In this case, the channel length, l ,
 equals a quarter wavelength, $\Lambda/4$.

That is,

$$c = \frac{\Lambda}{T} = \frac{4l}{T} = \sqrt{gh}$$

$$T = \frac{4l}{\sqrt{gh}}$$



In general, for the higher nodes
 in an open channel:

$$T = \frac{4l}{n\sqrt{gh}}, \quad \text{for } n = 1, 3, 5, \dots$$

These calculations have an important
 practical use: avoid harbors
 with seiche resonance.

Storm surges

Storm-generated high water is called
a *storm surge*

It can be coupled with natural resonance
to give disastrous results.

Four effects may combine in various
proportions to create storm surges:

- wind stress
- high tide (especially spring tides)
- inverted barometer effect
[atmospheric loading]
- resonance

Example:

a hurricane can have a 100 mb
pressure difference. This would
yield a 1 m water level (due to
the inverted-barometer effect)

If the hurricane moves at \sqrt{gh} ,
there can be a coupled resonance

This is generally not a problem
in deep water, where

$$\sqrt{gh} \sim 200 \text{ m s}^{-1}$$

(or 400 knots,
or 720 km/hr)

But on the continental shelf,

$$\sqrt{gh} \sim 40\text{-}60 \text{ knots}$$

So there is more likelihood of a
hurricane-generated storm surge
on the shelf.

If the wind shift associated with
the hurricane has a speed $\sim \sqrt{gh}$,
there can be resonance
e.g., if the time for a 180° wind shift
corresponds to the seiche period

Long-period waves

For wave motions that have periods that begin to approach the inertial period,

$$\frac{12 \text{ hours}}{\sin f},$$

Earth's rotation must be taken into account

Assume:

- frictionless flow
- flow is barotropic: pressure gradients are due to free-surface displacement, h

Including the coriolis term, the balance of forces is:

$$\begin{aligned} \frac{\partial u}{\partial t} &= -g i_x + f v \\ &= -g \frac{\partial h}{\partial x} + f v \end{aligned}$$

$$\begin{aligned} \frac{\partial v}{\partial t} &= -g i_y - f u \\ &= -g \frac{\partial h}{\partial y} - f u \end{aligned}$$

where h is the displacement of the ocean surface

As well, the equation of continuity may be written:

$$\frac{\partial h}{\partial t} = -h \left(\frac{\partial u}{\partial x} + \frac{\partial v}{\partial y} \right) \text{ [see Knauss, p. 119]}$$

Solutions to these equations, which include the effects of Earth's rotation, give long-period waves:

- Kelvin waves
- Inertia Gravity (Poincaré) waves

The variation of the coriolis parameter with latitude gives yet another type of long-period wave:

- Rossby waves

Kelvin waves

Kelvin waves may exist where a lateral boundary occurs

If the boundary is east-west, the solutions to the above equations give:

$$h = h_0 e^{-fy/\sqrt{gh}} \cos(kx - wt)$$

$$= h_0 e^{-\frac{y}{R_d}} \cos(kx - wt)$$

where

$$R_d = \frac{\sqrt{gh}}{f} \text{ is the}$$

Rossby radius of deformation,
the transverse distance over which
Kelvin waves have an effect

See Knauss, Box 10.1, p. 225

The wave speed is

$$c = \sqrt{gh} = c_g$$

The lateral boundary (wall) is on the right in the Northern Hemisphere; on the left in the Southern

Kelvin waves travel around the boundaries of an ocean basin:
counter-clockwise (NH)
clockwise (SH)

The equator, where f changes sign, acts as a boundary along which, Kelvin waves propagate eastward

Kelvin waves have their maximum amplitude along the boundary and die off at a distance approximately that of R_d :

For deep water, ($h = 5000\text{m}$) $R_d \sim 2200 \text{ km}$

For a shallow sea, ($h = 100\text{m}$), $R_d \sim 300 \text{ km}$

Kelvin waves are often associated with tides.

Inertia gravity waves

For inertia gravity waves, the wave speed is

$$c_i = \frac{\sqrt{gh}}{\sqrt{1 - \left(\frac{f}{w}\right)^2}} \quad \boxed{\text{Knauss, p. 226}}$$

Note that the phase velocity depends on the wave frequency, so the waves are dispersive

Thus the group velocity is

$$V_i = \sqrt{gh} \sqrt{1 - \left(\frac{f}{w}\right)^2}$$

To exist, the wave frequency, w , must be greater than the coriolis parameter, f

That means that the wave period cannot be longer than the half-pendulum day

As the frequency, w , gets larger, the phase and group velocities approach those of a normal shallow-water wave, \sqrt{gh}

Rossby waves

The change of the coriolis parameter, f , with latitude is the factor behind Rossby or planetary waves

Let the coriolis parameter be described by a constant value and a term that varies linearly in the y -direction:

$$f = f_0 + by$$

Then the equations of motion become:

$$\begin{aligned} \frac{\partial u}{\partial t} &= +(f_0 + by)v - g \frac{\partial h}{\partial x} \\ \frac{\partial v}{\partial t} &= -\underbrace{(f_0 + by)}_{\text{coriolis force}} u - \underbrace{g}_{p g f} \frac{\partial h}{\partial y} \end{aligned}$$

For these waves with horizontal motion,
the term b provides the
restoring force, rather than gravity

The restoring force can be understood
by considering the conservation
of potential vorticity.

Recall that

$$\frac{d}{dt} \left(\frac{f + \alpha}{Z} \right) = 0$$

Consider a column of water of constant
layer depth, Z , and with zero
relative vorticity, α

Displacing the column northward increases
the planetary vorticity, f , so α must
decrease, imparting a clockwise rotation

The northern side of the column will
have a coriolis force southward,
while the southern side will have a
weaker coriolis force northward;
weaker because f increases northward

Thus, there will be a net southward
restoring force on the column of water

Rossby waves have a phase speed:

$$C_R = - \frac{b}{k^2 + \frac{f^2}{gh}}$$

which is always westward

For large values of k (short wavelength,
the phase speed is slow, and
the period can be very long

Internal waves

Internal waves occur on surfaces
between different density layers
in the sea.

The density in the two layers
is generally nearly the same.

The dispersion relation is:

$$c^2 = \frac{(r_2 - r_1) \frac{g}{k}}{r_2 \coth kh_2 + r_1 \coth kh_1}$$

If $r_2 \gg r_1$, this becomes

$$c^2 = \frac{g}{k} \tanh kh$$

Which is simply what we had earlier
for surface waves on the air-sea interface.

For deep-water (short) waves,

$$\coth kh \Rightarrow 1,$$

and

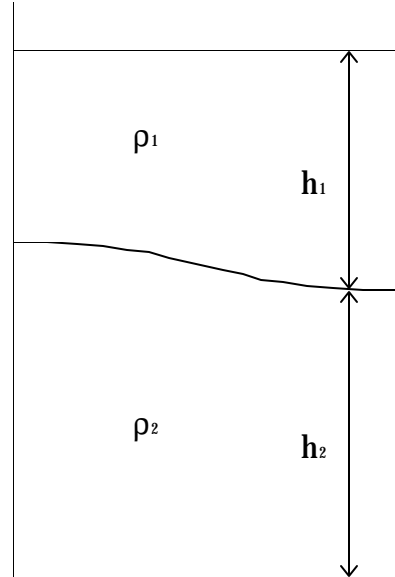
$$c^2 = \frac{g}{k} \left(\frac{r_2 - r_1}{r_2 + r_1} \right)$$

Since $\frac{r_2 - r_1}{r_2 + r_1} \ll 1$,

these waves have phase speeds that
are much smaller than those
for corresponding surface waves.

e.g., for $\frac{r_2 - r_1}{r} = \frac{\Delta r}{r} = 2 \times 10^{-3}$,

the ratio between internal and surface speeds
is $\sim 1/30$.



For shallow-water (long) waves,

$$\coth kh \Rightarrow 1/kh,$$

and the dispersion relation becomes

$$c^2 = g \frac{h_2 h_1}{h_2 + h_1} \frac{r_2 - r_1}{r_2}$$

The term $g \frac{r_2 - r_1}{r_2} = g \frac{\Delta r}{r}$

is often called “reduced gravity”

Again, the phase speeds are much smaller than for surface waves.

e.g., for $\frac{\Delta r}{r} = 2 \times 10^{-3}$,

the ratio between internal and surface wave speeds is $\sim 1/45$.

For a thin upper layer over a deep lower layer (like river outflow)

i.e., $h_1 < L/20$

and $h_2 > L/2$,

$$\coth kh_1 \Rightarrow \frac{1}{kh_1}$$

$$\coth kh_2 \Rightarrow 1$$

Giving:

$$c^2 = \frac{r_2 - r_1}{r_1} gh_1$$

The speed of all these waves is low, and their amplitude can be large.

The true ocean is seldom two-layer, as assumed in deriving these equations. The ocean is generally continuously stratified and internal waves occur throughout the water column

Internal-wave frequency limits

Internal waves occur over a range of frequencies whose high-frequency limit is related to the static stability.

This limit is the Brunt-Väisälä frequency, (discussed in Lecture 1):

$$N^2 = -\frac{g}{r} \frac{\rho_s}{\rho_z}$$

which gives a typical period in minutes

The low-frequency limit is the inertial frequency,

$$f = 2\Omega \sin\phi$$

which typically gives a period in hours

Measurements of internal waves

Fig 10- 2 A current-measuring device

(Ross 1970), Fig. 4-40

This is a Savonius-rotor current meter, being shackled into a deep-sea mooring line.

Fig 10- 3 Time series of currents at Site D

Fig. 5

These time series (of u and v velocity components) were obtained from a current meter of the type shown in the previous Figure. Can you identify the major oscillations that appear in the record?

Fig 10- 4 Spectrum of currents at Site D

(Fofonoff and Webster 1971), Fig. 6

This is the power spectrum for the measurements shown in the previous Figure. This may be considered a spectrum of internal waves. Spectrum peaks can be seen at semi-diurnal, diurnal, and inertial frequencies. Which peak is which? Why is no peak apparent at the Brunt-Väisälä frequency?

Fig 10- 5 Spectrum of currents at 100 m depth (Fofonoff and Webster 1971), Fig. 11

This power spectrum is from a much longer record than that shown in the previous Figure and consequently the lower frequencies are better resolved.

Internal waves may be generated by tides interacting with the continental shelf

Internal waves may break and thus can be important in deep-sea mixing and turbulence

Tidal forces

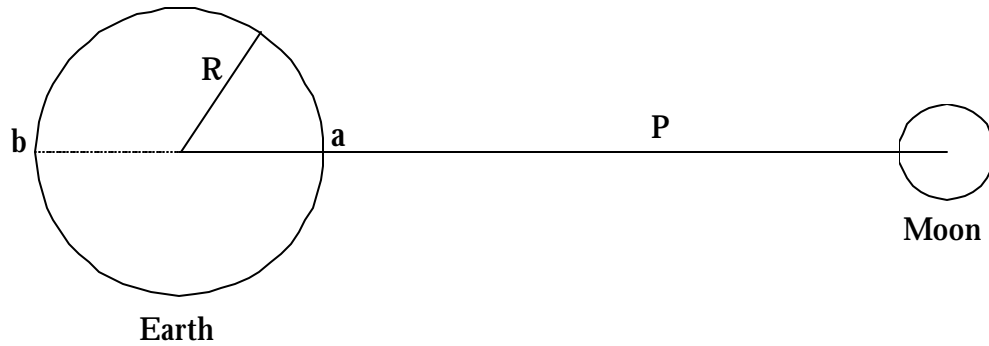
Tides are produced by the differential forces of the sun and moon.

We will look at a simplified model using the earth-moon system, with a balance between earth-moon gravitation and centrifugal acceleration of both.

The differential force arises because centrifugal force is the same at all points on earth, but gravitational attraction varies slightly with position

The gravitational force of the moon (which varies on Earth depending on distance from the moon) on a particle of mass m at a point, a , is:

$$F_a = G \frac{Mm}{(P - R)^2}$$



where:

G is the gravitational constant
 $= 6.67 \times 10^{-11} \text{ N kg}^{-1} \text{ m}^2$

M is the mass of the moon

P is the earth moon distance

R is the radius of the earth

The centrifugal force, F_c on a particle of mass m at all points on Earth, including point a , is:

$$F_c = G \frac{Mm}{P^2}$$

Thus, the imbalance at the point, a , is:

$$\begin{aligned} F_a - F_c &= G \frac{mM}{(P-R)^2} - G \frac{mM}{P^2} \\ &= \frac{2PR - R^2}{P^4 - 2P^3R + P^2R^2} GmM \end{aligned}$$

since $P \sim 60R$,

higher-order terms can be ignored and the equation can be simplified to

$$F_a - F_c \cong + \frac{2R}{P^3} GMm$$

At point b ,

a similar argument gives:

$$F_b - F_c \cong - \frac{2R}{P^3} GMm$$

These tide-generating forces vary inversely
as the cube of the distance, while the
gravitational attraction varies
as the square of the distance

Fig 10- 6 Tide-generating forces

(Pond and Pickard 1983), Fig. 13.3

This sketch summarizes the tide-producing
forces. Note the tidal bulge on the side of
Earth facing towards the moon as well as
on the side facing away.

The mass of the sun is
 2.5×10^7 times greater than
that of the moon.
but the distance is 400 times greater.

So the moon's tidal forces are about
twice those of the sun.

When the sun and moon are
in opposition or *conjunction*
the tide-generating forces are additive,
giving maximum tidal ranges,
known as *spring tides*

When the sun and moon are in *quadrature*,
the tide-generating force of the sun
works at right angles to that of the moon,
giving minimum tidal range,
known as *neap tides*

The time between successive spring tides
is about two weeks

The moon and sun are not
above the equator at all times

The earth's axis is tilted 23.5°
relative to its plane of revolution
about the sun (the *ecliptic*)
(We thus experience seasons)

The plane of the moon's orbit
 is at an angle of 5° to the ecliptic
 which rotates (or *precesses*)
 with a cycle of 18.6 years

The situation is complex
 The effect is that tidal bulges
 will rarely be aligned with the equator

Furthermore, as the earth rotates daily,
 the two high tides will generally
 be of unequal amplitude

Fig 10- 7 Unequal tides

(Thurman 1991), Fig 10-11

Note that the observer sees about two tides
 per day, but that generally one is higher
 than the other.

Equilibrium theory of the tides

We know the tidal forces
 Why not simply use them
 to compute the equilibrium tide?

There are a number of tidal-forcing constituents
 For example:

Symbol	Name	Period (solar hours)	Relative Amplitude
M_2	Principal lunar semi-diurnal	12.42	100
K_1	Lunar-solar diurnal	22.93	58
S_2	Principal solar semi-diurnal	12.00	47
O_1	Principal lunar diurnal	25.82	42

Assume Earth is covered with water
 of uniform depth
 giving predicted values of:

maximum lunar tide	0.55 m
maximum solar tide	0.24 m
maximum tide	0.79 m

The maximum tide occurs when
the sun and moon are in line

But, the observed tides don't have
the proper phase and amplitude
to match such a calculation

The amplitudes are
much greater than predicted
The phases don't match predictions
of times of high and low water

Why?

= Tides are dynamic
long waves are driven by
periodic fluctuations of the tidal forces

Also, the water depth in the ocean is not uniform

The problem of the equilibrium tide is to:

- relate a known driving force
- to a series of interconnected basins
- each with its own natural frequencies,
- each with its own frictional characteristics

i.e., \sqrt{gh} is variable throughout the ocean
and the ocean basins are irregular

We would need an ocean that is
21 km deep to accommodate
a wave that would take 12.4 hours
to travel halfway around the earth

At 21 km depth, there would be resonance.

But the actual average ocean depth ~ 4 km.

Using simplified ocean basin models
and large computers,
predictions based on dynamical theory
are giving promising results

Observed ocean tides

Maps of observed tides can be constructed from observations collected around the shores of oceans and on islands

Fig 10- 8 Cotidal lines for M₂ - global

IMG/LEGI

[sirius-ci.cst.cnes.fr:8090/images/information/applications/science/world/ocean_tides.gif]

The cotidal lines show the points having equal phase (in this case for the M₂ tide) Note the rotation of the tidal height around the amphidromic points.

Fig 10- 9 Semidiurnal M₂ tide - Atlantic, amphidromic points Knauss, Fig. 10.16

The cotidal lines do not show the amplitude of the tide, which is zero at the amphidromic points.

Fig 10- 10 Cotidal lines, Delaware Bay

(Polis and Kupferman 1973), Fig. 6

Here the cotidal lines are called “isochrons”. Why are they different for high and low tides?

Fig 10- 11 Cotidal lines, Gulf of Maine

(Redfield 1980), Fig. XI-1

Note both *cotidal* (solid) and *corange* (dashed) lines. The tidal ranges up the Bay of Fundy [to the right] becomes the largest in the world.

Fig 10- 12 Refraction of tidal wave, Gulf of Maine

(Redfield 1980), Fig. XI-3

Clearly, the bottom topography plays a role in refracting the tidal wave.

Fig 10- 13 Mean range of tides, US east coast

(Redfield 1980), Fig. XI-3

Along the US east coast the tidal ranges are generally between 3 and 5 feet.

Tidal Prediction

The classical method of tidal prediction
is based on harmonic analysis

Decompose the tide
into its major components
(as in the Table above)

Use the value of those components
measured at a given location
to reconstruct the tide at that location

To predict,
compute the components
add them up to get predictions

Fig 10- 14 Principal tidal harmonic components

Knauss, Table 10.1

The M_2 tide (period 12.42 hours) is usually
the dominant component.

Fig 10- 15 Sample tidal curves

(Defant 1961), Fig. 123

Note that (in spite of what was said in the
box above) the dominant tidal
components may vary according to
location. What processes might account
for this?

Fig 10- 16 Computation of the tide at Pula (Croatia)

Knauss, Fig. 10.15

This example shows how the summation of
tidal components can produce a
reasonably good approximation to the
observed tide.

Tidal prediction through summing
the components generally
gives good predictions,

But the process can be in error because of:

- winds
- inverted barometer effect
- (1mb atmos pressure \Rightarrow 1 cm water height)
- heating and cooling
- ocean currents

Tidal-height predictions, are available
in the Library (Ref. 54, for example)

The government-produced
NOS/NOAA Tide Tables, have been
discontinued in favor of the
World Wide Web, CD-ROM's,
and private enterprise

for tide predictions, try
<http://tbone.biol.sc.edu/tide/sitesel.html>

Fig 10- 17 Tidal differences for Roosevelt Inlet

(Herzog and Ellison 2000)

When is high tide at Lewes (Roosevelt
Inlet) today?

Fig 10- 18 Tidal current tables, Roosevelt Inlet

(Herzog and Ellison 2000)

When will the flood current occur today
between the jetties at Roosevelt Inlet?
What will be the like strength and
direction of the current?

Fig 10- 19 Delaware River Distance and Tide Table

(Pilot's Association for the Bay and River Delaware)

This is a copy of a page from the little book
used by Delaware Bay pilots. Note the
progression of the tide up the Bay from
Cape Henlopen to Chestnut St. wharf in
Philadelphia. What controls the time of
this progression?

Tidal currents

Water motion associated with
the tides can be
~ 2 to 5 cm/s in the open ocean

Fig 10- 20 Tidal current ellipse

Knauss, Fig. 10.17

In this case, the currents are relatively
strong. [1 knot = 0.5125 m s⁻¹]

Tidal currents can be intense
in coastal waters
Particle speed in a shallow-water wave is

$$u = c \frac{A}{h}$$

where $c = \sqrt{gh}$

so that

$$u = A \left[\frac{g}{h} \right]^{\frac{1}{2}}$$

If A is constant,
then u increases as h decreases

Resonance is possible,
e.g., Bay of Fundy

Altimetric measurement of ocean currents

If the ocean were at rest
sea level would be a surface
of constant gravitational potential
= the *geoid*

However, the ocean surface
does not match the geoid

Deviations from the geoid are caused
(among other effects) by

- surface geostrophic currents
- tides

Thus, ocean topography can be used
to estimate ocean currents

Recall that

$$v_s = \frac{g i}{f},$$

where $i = \frac{\eta h}{\eta x} = \text{slope}$

We can use orbiting altimeters
to determine i , and thus v_s

Fig 10- 21 Satellite altimeter

Fig. 1

The accuracy of the topex-poseidon
altimetric satellite is nearly 1 cm.

Fig 10- 22 Ground track of altimetric satellite

Fig. 2

The area of the earth that is covered and the
repeat time have to be carefully chosen to
be sure that there is no aliasing of tides
onto critical periods (like the annual, for
instance.)

This procedure can be used on a global scale,
and is a key observing component of the
World Ocean Circulation Experiment (woce)

See, for example, the “movies” on the
World Wide Web at

www-mount.ee.umn.edu/~dereklee/micom_movies/srfhgt.html

Fig 10- 23 Kinetic energy of geostrophic currents

Fig. 16

Where and why is the kinetic energy of
surface geostrophic currents the greatest?
Why is the Antarctic Circumpolar Current
not shown here?

Altimetric measurements and hydrographic station data can be combined.

Recall the thermal wind equation:

$$\frac{\partial v}{\partial z} = -\frac{g}{rf} \frac{\partial r}{\partial x}$$

Which can be integrated to give:

$$v = \frac{g}{f} \int_{z_0}^{-z} \frac{1}{r} \frac{\partial r}{\partial x} + v_0$$

where v_0 is the reference velocity.

i.e., knowing $\frac{\partial r}{\partial x}$ and a reference velocity (determined from an altimeter), the absolute vertical profile of currents can be determined.

Lecture 9 Figures

Fig 10- 1	Domestic seiche	Calvin & Hobbes
Fig 10- 2	A current-measuring device	(Ross 1970), Fig. 4-40
Fig 10- 3	Time series of currents at Site D	Fig. 5
Fig 10- 4	Spectrum of currents at Site D	(Fofonoff and Webster 1971), Fig. 6
Fig 10- 5	Spectrum of currents at 100 m depth	(Fofonoff and Webster 1971), Fig. 11
Fig 10- 6	Tide-generating forces	(Pond and Pickard 1983), Fig. 13.3
Fig 10- 7	Unequal tides	(Thurman 1991), Fig. 10-11
Fig 10- 8	Cotidal lines for M2 - global	IMG/LEGI
Fig 10- 9	Semidiurnal M2 tide - Atlantic, amphidromic points	Knauss, Fig. 10.16
Fig 10- 10	Cotidal lines, Delaware Bay	(Polis and Kupferman 1973), Fig. 6
Fig 10- 11	Cotidal lines, Gulf of Maine	(Redfield 1980), Fig. XI-1
Fig 10- 12	Refraction of tidal wave, Gulf of Maine	(Redfield 1980), Fig. XI-3
Fig 10- 13	Mean range of tides, US east coast	(Redfield 1980), Fig. XI-3
Fig 10- 14	Principal tidal harmonic components	Knauss, Table 10.1
Fig 10- 15	Sample tidal curves	(Defant 1961), Fig. 123
Fig 10- 16	Computation of the tide at Pula (Croatia)	Knauss, Fig. 10.15
Fig 10- 17	Tidal differences for Roosevelt Inlet	(Herzog and Ellison 2000)
Fig 10- 18	Tidal current tables, Roosevelt Inlet	(Herzog and Ellison 2000)
Fig 10- 19	Delaware River Distance and Tide Table	(Pilot's Association)
Fig 10- 20	Tidal current ellipse	Knauss, Fig. 10.17
Fig 10- 21	Satellite altimeter	Fig. 1
Fig 10- 22	Ground track of altimetric satellite	Fig. 2
Fig 10- 23	Kinetic energy of geostrophic currents	Fig. 16

References

- Defant, Albert (1961). *Physical Oceanography, Vol II*, Macmillan, New York, 598 pp.
- Fofonoff, N.P. & F. Webster (1971). Current measurements in the western Atlantic. *Phil. Trans. R. Soc. Lond. A* **270**: 423-436.
- Herzog, Carl & Ben Ellison (2000). *Reed's Nautical Almanac, North American East Coast*. 27th, Thomas Reed, Boston.
- Pilot's Association for the Bay and River Delaware ((Annual Pub.)). *Tides and Currents*, Philadelphia.
- Polis, D.F. & S.L. Kupferman (1973). *Physical Oceanography*. Newark, DE, Univ. of Delaware: 143.
- Pond, Stephen & George L. Pickard (1983). *Introductory Dynamical Oceanography*. 2nd, Pergamon, Oxford, 329 pp.
- Redfield, Alfred C. (1980). *The tides of the waters of New England and New York*, Marine Science International, Boston, 108 pp.
- Ross, David A. (1970). *Introduction to Oceanography*, Appleton-Century-Crofts, New York.
- Thurman, Harold V. (1991). *Introductory Oceanography*. 6th, McMillan, New York, 526 pp.